

MICROCRACK NUCLEATION IN Ti_3Al DUE TO DISLOCATION INTERACTIONS

Liudmila Yakovenkova and Lidia Karkina

Institute of Metal Physics, Russian Academy of Sciences, Ekaterinburg, 620219, GSP-170, Russia

Received: February 03, 2008

Abstract. The reactions of interaction between the superdislocations, which accomplish deformation in the basal, prism and pyramidal (I and II types) planes in the single crystal of Ti_3Al are examined. Interaction modes, which lead to the formation of dislocation barriers - the microcrack nucleation are established. The force and energy conditions for the formation of microcracks are examined. The classification of the types of microcracks in the dependence on the orientation of the deformation axes of the single crystals is carried out. The regions of stereographic triangle, the characterized by preferred type crack openings are found.

1. INTRODUCTION

The intermetallic compound Ti_3Al with the ordered hexagonal superlattice DO_{19} , is the main component of a number of the single-phase and two-phase alloys, promising for the practical application as high-temperature strength and high-temperature oxidation-resistant materials. Similar to many intermetallic compounds, Ti_3Al possesses low plasticity at room temperature, which prevents their active practical application. Depending on the conditions for experiment (temperature, deformation rate, orientation of the axis of deformation, etc., there realizes the slip of \mathbf{a} , $\mathbf{c}+\mathbf{a}$, $2\mathbf{c}+\mathbf{a}$ superdislocations in the basal, prism and pyramidal plane. The lightest mode of the deformation of Ti_3Al is prismatic slip $1/3\langle 11\bar{2}0 \rangle\{1\bar{1}00\}$. In the basal plane (0001) the deformation also is accomplished by superdislocations with the vector of Burgers $1/3\langle 11\bar{2}0 \rangle$ [1-5].

As a rule, for the ordered alloys high strength properties are combined with the low plastic char-

acteristics. For example, in the intermetallic compounds with the superlattice $L1_2$ the peak in the curve of the dependence of $s_y(T)$ is accompanied by a plasticity minimum near the peak temperature. This correlation is violated for Ti_3Al : for single crystals oriented for $1/3\langle 11\bar{2}0 \rangle\{1\bar{1}00\}$ and $1/3\langle 11\bar{2}0 \rangle(0001)$ slip, the values of elongation differ into hundred times. The mechanism of the shift type microcracks formation due to interaction of screw superdislocations in the basal plane slip band is proposed into [1,2]. The model is based on the results of the computer simulation of superdislocations core structure in Ti_3Al [3,4]. Formation and coalescence of microcracks leads to brittle failure of Ti_3Al single crystal oriented for the basic slip. The possibility of the microcracks nucleation in Ti_3Al as a result of dislocation reactions is shown in [5] with the electron-microscopic study. Fig. 1 shows the micrograph, which demonstrates the type of microcrack formation as a result of dislocation interaction. One can see that a microcrack

Corresponding author: Liudmila Yakovenkova, e-mail: yakovenkova@imp.uran.ru

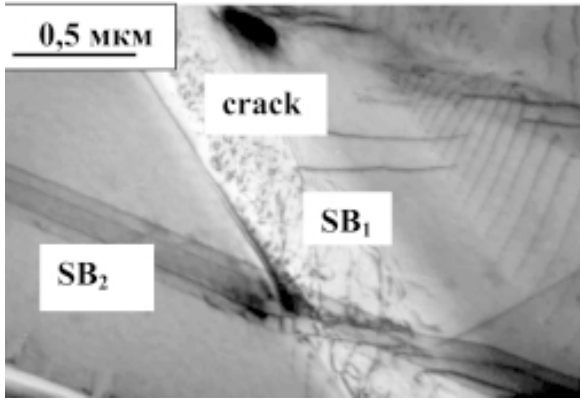


Fig. 1. Bright-field image of a microcrack due to room temperature indentation of Ti_3Al . Slip bands SB_1 ($1/3[\bar{1}2\bar{1}6](1\bar{1}\bar{1}1)$), SB_2 ($1/3[2\bar{1}\bar{1}0](01\bar{1}0)$) and a microcrack in pyramidal plane are indicated

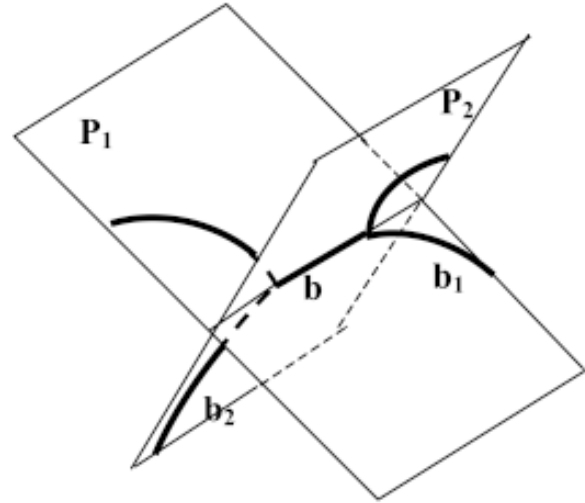


Fig. 2. Scheme of dislocation barrier formation. A microcrack appears due to the intersection of dislocations with the Burgers vectors b_1 and b_2 .

can nucleate at the line of intersection of $\{11\bar{2}1\}$ pyramidal and $\{01\bar{1}0\}$ prismatic planes.

The purpose of this investigation is the consecutive consideration of the nucleation microcrack geometry, which appears due to dislocation interactions taking into account all experimentally observed slip systems of superdislocations in Ti_3Al ; the calculation of interaction between blocked and glissile dislocations; conducting the detailed orientation dependence analysis of microcracks types and crystal characteristics. The force and energy conditions for the formation of microcracks are examined. The atomistic core structure of superdislocation was obtained as a result of calculations by the molecular dynamic method [6].

2. RESULTS

The dislocation reaction between the mobile dislocations along the intersection of their slip planes results to the dislocation barrier formation, which can cause the microcrack appearance (Fig. 2). Let us designate n_ξ - normal to the plane, which contains the summary vector of Burgers of the dislocations, which entered the dislocation reactions, and vector l is directed along the intersection of slip planes. The normal to the plane of possible microcrack is determined by relationship $[n_\xi \times l]$. The growth of the microcrack is ensured by the absorption of other dislocations under the action of external stresses and stresses, created by dislocation array. Interaction energy per unit of length

between two parallel interacting dislocations has the form [7]:

$$W = -\frac{G(\mathbf{b}_1 \times \xi)(\mathbf{b}_2 \times \xi)}{2\pi} \ln \frac{R}{R_0} - \frac{G[(\mathbf{b}_1 \times \xi)(\mathbf{b}_2 \times \xi)]}{2\pi(1-\nu)} \ln \frac{R}{R_0} - \frac{G[(\mathbf{b}_1 \times \xi)R][(\mathbf{b}_2 \times \xi)R]}{2\pi(1-\nu)R^2}, \quad (1)$$

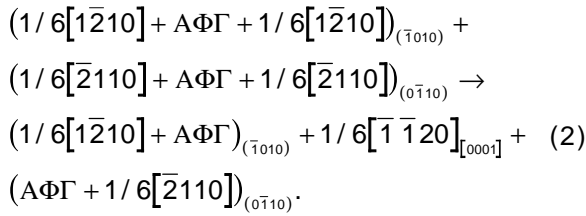
where b_1 , b_2 are the Burgers vectors of the interacting dislocations; ξ is the axis of the interacting dislocations, parallel to the intersection of the slip planes of these dislocations; R is the distance between the interacting dislocations; R_0 is a constant, which has dimensionality R ; G , n is the shear modulus and Poisson ratio. If the force of interaction between the dislocations ($F = -\partial W / \partial R$) $F > 0$, the dislocations are repelled, at $F < 0$ they are attracted. There are no long-range interaction between the dislocations if $F = 0$, but dislocation reaction can occur in the stress field of dislocation in array and external stresses.

Let us consider dislocation interactions taking into account the acting slip planes and Burgers vectors of the superdislocations, which accomplish plastic deformation in Ti_3Al . Fore types of dislocation interactions are possible:

- 1) between \mathbf{a} -superdislocations gliding in two prism planes or in prism and basal planes;
- 2) between \mathbf{a} -superdislocations in the basal plane and $2\mathbf{c}+\mathbf{a}$ superdislocations in the pyramidal planes of I and II type;
- 3) between \mathbf{a} -superdislocations in the prism planes and $2\mathbf{c}+\mathbf{a}$ superdislocations in the pyramidal planes of I and II type;
- 4) between $2\mathbf{c}+\mathbf{a}$ superdislocations, which glide in the pyramidal planes of I and II type.

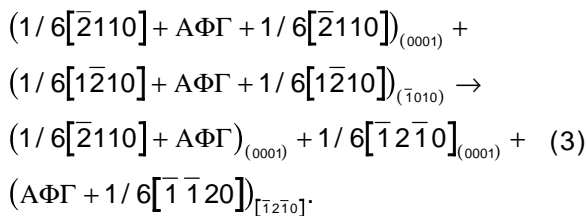
2.1. Dislocation reactions between \mathbf{a} -superdislocations

The typical dislocation reaction between split \mathbf{a} -superdislocations that glide in two intersecting prism planes takes the following form:



The resulting dislocation $1/6[\bar{1}\bar{1}20]$ lies along the direction $[0001]$ coinciding with the intersection prism planes line. This dislocation is mobile in the plane prism $(\bar{1}100)$, which does not coincide with the slip planes of reacting $\mathbf{a}/2$ – superdislocation. Slip of $1/6[\bar{1}\bar{1}20]$ dislocation in $(\bar{1}100)$ plane leads to the reaction, similar to 2, between remained $\mathbf{a}/2$ – superdislocation, which limit APB strip. As a result, \mathbf{a} – superdislocation with the Burgers vector $1/3[\bar{1}\bar{1}20]$ glides in the prism plane $(\bar{1}100)$. Thus, interaction \mathbf{a} – superdislocations in the prism planes does not lead to the microcracks nucleation.

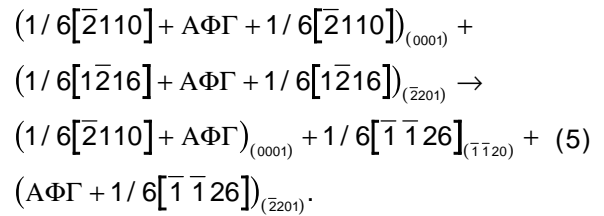
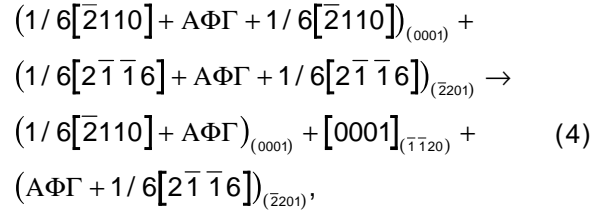
The typical dislocation reaction between split \mathbf{a} – superdislocations sliding in the intersecting basal and prism planes, takes the form:



The resulting dislocation with the Burgers vector $1/6[\bar{1}\bar{1}20]$ lies along the intersection line $[\bar{1}\bar{2}10]$ of the basal and prism planes. This dislocation is mobile in the basal plane (0001) . In such case for reaction (2), interaction of \mathbf{a} – superdislocations in the basal and prism planes does not lead to the formation of a microcrack.

2.2. Dislocation reactions between \mathbf{a} -superdislocations in the basal plane and $2\mathbf{c}+\mathbf{a}$ superdislocations in the pyramid planes

There are possible two different variants of the dislocation reactions between split \mathbf{a} -superdislocations in the basal plane and $2\mathbf{c}+\mathbf{a}$ -by superdislocations in the plane of I type pyramid:



The resulting dislocations have Burgers vectors $[0001]$ (reaction (4)) and $1/6[\bar{1}\bar{1}26]$ (reaction (5)); in both cases the axis direction is $[\bar{1}\bar{1}20]$. This configuration is a dislocation barrier; a possible plane of crack opening is (0001) . Let us note that at high temperatures of deformation ($T > 1024K$), the glide of dislocation with the vector of Burgers $[0001]$ was observed experimentally, whereas at lower temperatures these dislocations were blocked [8,9].

There are two possible ways of the dislocation reactions between interacting \mathbf{a} -superdislocations in the basal plane and $2\mathbf{c}+\mathbf{a}$ superdislocations in the pyramidal plane of II type:

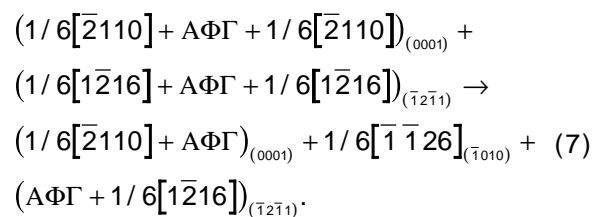
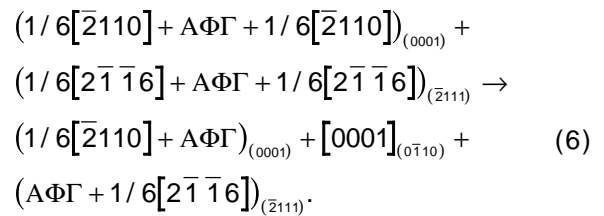


Table 1. Dislocation reactions and the expected planes of fracture for interaction of $2\mathbf{c}+\mathbf{a}$ superdislocations in pyramidal planes.

No	Slip systems of interacting dislocations	Burgers vectors of resultant dislocations	Orientation of star rod dislocation	Fracture plane expected
1	$1/3[11\bar{2}6](\bar{2}021)$ $1/3[2\bar{1}\bar{1}\bar{6}](\bar{2}02\bar{1})$	$[10\bar{1}0]$	$[1\bar{2}10]$	$(10\bar{1}0)$
2	$1/3[11\bar{2}6](\bar{2}021)$ $1/3[11\bar{2}\bar{6}](02\bar{2}1)$	$2^*1/3[11\bar{2}0]$	$[1\bar{1}02]$	$(11\bar{2}0)$
3	$1/3[11\bar{2}6](\bar{2}021)$ $1/3[1\bar{2}\bar{1}\bar{6}](02\bar{2}1)$	$[01\bar{1}0]$	$[1\bar{1}02]$	$\sim(13\bar{4}1)$
4	$1/3[11\bar{2}6](\bar{2}021)$ $1/3[1\bar{2}\bar{1}\bar{6}](\bar{2}201)$	$[01\bar{1}0]$	$[2\bar{1}\bar{1}6]$	$(01\bar{1}0)$
5	$1/3[11\bar{2}6](\bar{2}021)$ $1/3[1\bar{2}\bar{1}\bar{6}](\bar{2}\bar{2}01)$	$1/3[2\bar{1}\bar{1}0]$	$[01\bar{1}2]$	$(2\bar{1}\bar{1}0)$
6	$1/3[1\bar{1}\bar{2}6](11\bar{2}1)$ $1/3[1\bar{2}\bar{1}\bar{6}](1211)$	$[0\bar{1}10]$	$[2\bar{1}13]$	$(0\bar{1}10)$
7	$1/3[1\bar{1}\bar{2}6](11\bar{2}1)$ $1/3[1\bar{2}\bar{1}\bar{6}](1\bar{2}1\bar{1})$	$1/3[2\bar{1}10]$	$[0\bar{1}13]$	(2110)
8	$1/3[1\bar{1}\bar{2}6](11\bar{2}1)$ $1/3[1\bar{1}\bar{2}\bar{6}](\bar{2}021)$	$2^*1/3[1\bar{1}20]$	$[5\bar{7}26]$	$\sim(8.3.11.1)$
9	$1/3[1\bar{1}\bar{2}6](11\bar{2}1)$ $1/3[2\bar{1}1\bar{6}](\bar{2}021)$	$[1010]$	$[5\bar{7}26]$	(6391)
10	$1/3[1\bar{1}\bar{2}6](11\bar{2}1)$ $1/3[1\bar{2}\bar{1}\bar{6}](\bar{2}201)$	$1/3[2\bar{1}10]$	$[1.5.4.12]$	$(15.6.9.1)$
11	$1/3[1\bar{1}\bar{2}6](11\bar{2}1)$ $1/3[2\bar{1}1\bar{6}](\bar{2}201)$	$[1010]$	$[1.5.4.12]$	$\sim(11\bar{2}1)$

The axes directions of resulting dislocations are $\langle 1\bar{1}00 \rangle$, a possible plane of crack opening is (0001). Thus, for \mathbf{a} -superdislocations in basal plane and $2\mathbf{c}+\mathbf{a}$ -superdislocations in the pyramidal planes of I and II type, the microcrack opening in the basal plane (0001) is possible.

2.3. Dislocation reactions between \mathbf{a} -superdislocations in the prism planes of and $2\mathbf{c}+\mathbf{a}$ superdislocations in the pyramidal planes

There are possible three different variants interaction \mathbf{a} -superdislocations in the plane of prism and $2\mathbf{c}+\mathbf{a}$ -superdislocation in the pyramidal planes of I type:

$$\begin{aligned} & (1/6[\bar{2}110] + A\Phi\Gamma + 1/6[\bar{2}110])_{(0\bar{1}10)} + \\ & (1/6[2\bar{1}\bar{1}6] + A\Phi\Gamma + 1/6[2\bar{1}\bar{1}6])_{(\bar{2}201)} \rightarrow \\ & (1/6[\bar{2}110] + A\Phi\Gamma)_{(0\bar{1}10)} + [0001]_{(\bar{2}116)} + \quad (8) \\ & (A\Phi\Gamma + 1/6[2\bar{1}\bar{1}6])_{(\bar{2}201)}, \end{aligned}$$

$$\begin{aligned} & (1/6[1\bar{2}10] + A\Phi\Gamma + 1/6[1\bar{2}10])_{(\bar{1}010)} + \\ & (1/6[\bar{2}116] + A\Phi\Gamma + 1/6[\bar{2}116])_{(\bar{2}201)} \rightarrow \\ & (1/6[1\bar{2}10] + A\Phi\Gamma)_{(\bar{1}010)} + [1\bar{1}\bar{2}6]_{(\bar{1}2\bar{1}6)} + \quad (9) \\ & (A\Phi\Gamma + 1/6[\bar{2}116])_{(\bar{2}201)}, \end{aligned}$$

$$\begin{aligned} & (1/6[1\bar{2}10] + A\Phi\Gamma + 1/6[1\bar{2}10])_{(\bar{1}010)} + \\ & (1/6[\bar{2}116] + A\Phi\Gamma + 1/6[\bar{2}116])_{(\bar{2}201)} \rightarrow \\ & (1/6[1\bar{2}10] + A\Phi\Gamma)_{(\bar{1}010)} + [1\bar{1}\bar{2}6]_{(\bar{1}2\bar{1}0)} + \quad (10) \\ & (A\Phi\Gamma + 1/6[\bar{2}116])_{(\bar{2}0\bar{2}1)}. \end{aligned}$$

For reaction (10), the resulting dislocation with the vector of Burgers $1/6[2\bar{1}\bar{1}6]$ and axis $[1\bar{2}10]$ in pyramidal plane $(20\bar{2}1)$ I type is mobile.

Two different dislocation reactions for interacting \mathbf{a} -superdislocations in the prism plane and $2\mathbf{c}+\mathbf{a}$ superdislocations in the pyramidal planes of II type are possible:

$$\begin{aligned} & (1/6[\bar{2}110] + A\Phi\Gamma + 1/6[\bar{2}110])_{(0\bar{1}10)} + \\ & (1/6[2\bar{1}\bar{1}6] + A\Phi\Gamma + 1/6[2\bar{1}\bar{1}6])_{(\bar{2}\bar{1}\bar{1}1)} \rightarrow \\ & (1/6[\bar{2}110] + A\Phi\Gamma)_{(0\bar{1}10)} + [0001]_{(\bar{2}116)} + \quad (11) \\ & (A\Phi\Gamma + 1/6[2\bar{1}\bar{1}6])_{(\bar{2}\bar{1}\bar{1}1)}, \end{aligned}$$

$$\begin{aligned} & (1/6[1\bar{2}10] + A\Phi\Gamma + 1/6[1\bar{2}10])_{(\bar{1}010)} + \\ & (1/6[\bar{2}116] + A\Phi\Gamma + 1/6[\bar{2}116])_{(\bar{2}\bar{1}\bar{1}1)} \rightarrow \\ & (1/6[1\bar{2}10] + A\Phi\Gamma)_{(\bar{1}010)} + [1\bar{1}\bar{2}6]_{(\bar{1}2\bar{1}3)} + \quad (12) \\ & (A\Phi\Gamma + 1/6[\bar{2}116])_{(\bar{2}\bar{1}\bar{1}1)}. \end{aligned}$$

In both cases the resulting dislocation presents a dislocation barrier. Thus, the microcrack formation

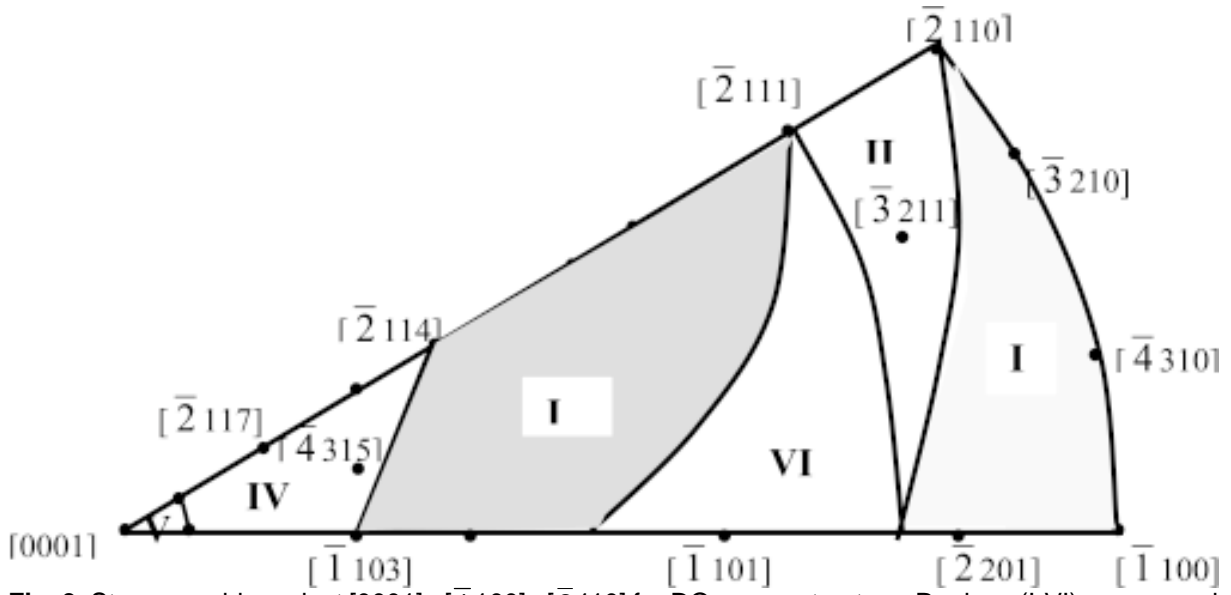


Fig. 3. Stereographic project $[0001] - [1\bar{1}100] - [2\bar{1}10]$ for DO_{19} superstructure. Regions (I-VI) correspond to different superdislocation interacting slip systems.

in the basal planes (0001) and the pyramidal planes $(03\bar{3}1)$ and $(\bar{1}\bar{2}32)$ for interaction \mathbf{a} -superdislocations of the prism plane and $2\mathbf{c}+\mathbf{a}$ -superdislocations of the pyramidal planes of I and II type is possible.

2.4. Dislocation reactions between $2\mathbf{c}+\mathbf{a}$ -superdislocations in different pyramidal planes of I or II type

There are realized 17 variants of dislocation reactions for interaction of $2\mathbf{c}+\mathbf{a}$ -super-dislocation in the pyramidal planes of I and/or II type. The annihilation reaction for screw superdislocations of opposite sign is the simplest reaction of interaction (two different variants). Two interaction types of $2\mathbf{c}+\mathbf{a}$ -superdislocations lead to formation and the \mathbf{A} -superdislocation gliding in the basal plane:

$$\begin{aligned}
 & (1/6[11\bar{2}6] + A\Phi\Gamma + 1/6[11\bar{2}6]) + \\
 & (1/6[11\bar{2}6] + A\Phi\Gamma + 1/6[11\bar{2}6]) \rightarrow \\
 & (1/6[11\bar{2}6] + A\Phi\Gamma) + 1/3[11\bar{2}0] + \quad (13) \\
 & (A\Phi\Gamma + 1/6[11\bar{2}6]).
 \end{aligned}$$

If interacting $2\mathbf{c}+\mathbf{a}$ -superdislocation belong to planes $(2\bar{0}21)$ and $(20\bar{2}1)$, the axis of the result-

ing dislocation coincides with the direction $[1\bar{2}10]$, i.e., in the basal plane 60° \mathbf{a} -super-dislocation will glide. In opposite case, the slip plane of reacting $2\mathbf{c}+\mathbf{a}$ -superdislocations is $(\bar{1}\bar{1}21)$ and $(11\bar{2}1)$, and on the line of their intersection an edge \mathbf{a} -superdislocation is formed. Slip of \mathbf{a} -superdislocation in the basal plane weakens its repulsion to remained $\mathbf{c}+\mathbf{a}/2$ -superpartial dislocations in the initial pyramidal planes. This leads to their recombination and formation of the second \mathbf{a} -superdislocation in the basal plane; a barrier is not forming.

There are two variants, when a dislocation barrier is not formed; they correspond to the dislocation reaction between $2\mathbf{c}+\mathbf{a}$ -superdislocations in pyramidal planes of I and II type $((20\bar{2}1)$ and $(11\bar{2}1)$), or in two planes $((20\bar{2}1)$ and $(02\bar{2}1)$) I type. The Burgers vector $1/6[1\bar{2}10]$ and the resulting dislocation line $[1\bar{2}26]$ in both cases belong in $(20\bar{2}1)$ plane. The other 11 possible interaction types of $2\mathbf{c}+\mathbf{a}$ -superdislocations in the pyramidal planes result in the star rod dislocation and microcracks formation. The Burgers vectors, axis of the star rod dislocations and the expected microcracks opening planes are represented in Table 1.

The classification of the microcrack types, which are formed due to interaction of dislocations, made

it possible to determine five regions of the axes of the deformation orientations of single crystals (Fig. 2). Near the line $[\bar{1} 100] - [2 110]$ of stereographic project (region II), it is possible to expect the high degree of deformation before the destruction, since they do not result in the dislocation barriers formation. In the narrow region of orientations near $[0001]$ ($< 10^\circ$, region V), the interaction of $2\mathbf{c}+\mathbf{a}$ -superdislocations leads to the microcrack formation in the pyramidal planes. In the remaining part of the stereographic project, the microcracks are formed predominantly in the basal plane; in the regions II, III, a shear type microcrack formed, in the regions I, IV, cracks of both shear type and normal opening are present.

3. CONCLUSIONS

The possible interaction reactions between the superdislocations, which accomplish deformation in the single-crystal Ti_3Al are considered. It was established that the interaction \mathbf{a} -superdislocations in the basal or prism planes does not lead to the stair rod dislocations (barriers) and microcracks formation. The interaction of \mathbf{a} -superdislocations of the basal plane and $2\mathbf{c}+\mathbf{a}$ superdislocations of the pyramidal planes of type I and II, result in fracture in the basal plane (0001). The basal or pyramidal planes are the possible fracture planes due to interaction of \mathbf{a} -superdislocations in the prism plane and $2\mathbf{c}+\mathbf{a}$ superdislocations in the pyramidal planes. It is shown that interaction of $2\mathbf{c}+\mathbf{a}$ -

superdislocations in different pyramidal planes of type I and/or type II, leads to the formation of microcracks in the prism and pyramidal planes (Table 1). The force and energy conditions for the formation of microscopic cracks are examined. The classification of the microcracks types formed due to dislocation interactions is carried out; the types depending on the orientation of the deformation axes of the single crystals. The regions of stereographic triangle, which characterized by preferred type crack openings are determined.

REFERENCES

- [1] Y. Umakoshi, T. Nakano and T. Takenaka // *Acta Metall. Mater.* **41** (1993) 1149.
- [2] Y. Minonishi // *Phil. Mag. A.* **63** (1991) 1085.
- [3] Y. Minonishi and M.N. Yoo // *Phil. Mag. Letters* **61** (1990) 203.
- [4] E.V. Panova, L.E. Karkina and E.P. Romanov // *Phys. Met. Metallogr.* **75** (1993) 166.
- [5] L.E. Karkina, O.A. Elkina and L.I. Yakovenkova // *Physics of Solid State* **49** (2007) 1680.
- [6] L.I. Yakovenkova, L.E. Karkina and M.Ya.Rabovskaya // *Technical Physics* **73** (2003) 60.
- [7] J. Hirth and J. Lothe, *Theory of Dislocations* (N.Y., 1972).
- [8] S.A. Court, J.P.A. Lofvander, M.H. Loretto and H.L. Fraser // *Phil. Mag.* **59A** (1989) 280.
- [9] S.M.L. Sastry and H.A. Lipsitt // *Acta Metallurgica* **25** (1977) 1279.